Climatic Lightning activity and its Correlations with Meteorological Parameters in South China

Dong Zheng[1,2*], Yijun Zhang[1,2], Luwen Chen[3]

1. State Key Laboratory of Severe Weather, Chinese Academy of Meteorological Sciences, Beijing, China
2. Laboratory of Lightning Physics and Protection Engineering, Chinese Academy of Meteorological Sciences, Beijing, China
3. Lightning Protection Center of Guangdong Province, Guangzhou, China

ABSTRACT: The lightning activity and its correlations with meteorological parameters in South China were studied in this paper, based on the cloud-to-ground (CG) lightning, total lightning, precipitation and reanalysis data. We analyzed the temporal and spatial characteristics of the lightning activity, compared the lightning activities (including positive CG lightning and great-current CG lightning) over the land and the offshore water, and in the summer (from May to September) and other seasons, and revealed the prominent differences. The precipitation was found to have better spatial correlation with the great-current CG lightning. The rain-yields per flash (RPF) are of the order of 10^8 kg fl^{-1} in whole analysis region. The spatial distribution of RPF is opposite to that of the density of total CG lightning, which can be best described by the power function with the correlation coefficient of -0.969. CAPE shows the most outstanding relationship with the lightning in monthly variation among the meteorological parameters associated with atmospheric stratification. We found the power-function correlation is better than linear correlation to describe the relation between lightning and CAPE, with the correlation coefficients being evenly distributed and popularly above 0.8 in whole region.

INTRODUCTION

Lightning activity has an important effect on human life with the destructiveness caused by its randomness, large current and strong electromagnetic radiation. Lightning activity is also an important agency indicating the convections and even climatic change. Along with the development of lightning detection technology and the expansion of lightning detection network, lightning data has been widely applied in the fields of meteorology, climate, lightning protection and so on. In this paper, we use the cloud-to-ground (CG) lightning data observed by Guangdong Lightning Location System (GLLS) that has the longest continuous observation in China, total lightning and precipitation data provided by the Tropical Rainfall Measuring Mission (TRMM) team, and meteorological reanalysis date of ERA provided by European Center for Medium-Range Weather Forecasts (ECMWF) to study the lightning activity and its relations with meteorological parameters in South China. The analysis period is from 2001 to 2012.

* Contact information: Dong Zheng, Chinese Academy of Meteorological Sciences, Beijing, China,
Email: zhd@cams.cma.gov.cn

OBSERVATION AND DATA

GLLS was first constructed in 1996 and form the network consisting of 16 time-of arrival/magnetic direction finder in 2000 (see Figure 1). Therefore, in order to keep the consistence of the data, the initial year of the CG data in study was chosen as 2001. The overall detection efficiency and median average error of location accuracy of GLLS based on the data of the transmission line faults caused by lightning is approximately equal to 86% and 1.0 km, respectively, in 1999 when there were temporarily 14 sensors in the network [Chen S. et al. 2002]. Chen L. et al. [2012] evaluated the performance of GLLS, based on observation data of the triggered lightning flashes obtained in Conghua, Guangdong and natural lightning flashes to tall structures obtained in Guangzhou, Guangdong. They reported the flash detection efficiency was about 94%, mean location error was about 710 m, and mean percentage error of peak current estimation was 16.3%.

The original data which was associated with the return stork was combined to form lightning flash data, according to the criterion that the adjacent return strokes in one flash should be within 0.5-s interval, 10-km distance and with same polarity. The average position of the return strokes located by the most sensors was specified as that of the flash. The maximum peak current among the return strokes was specified as that of the flash. In any content related to the current of flashes in this paper, the flash was located by at least 3 sensors. Furthermore, the positive cloud-to-ground (PCG) flashes with current smaller than 10 kA was removed from the data, due to they might be the misjudgement of cloud lightning [Cummins et al. 1998]. The CG lightning with peak current larger than 50 kA, 75 kA, and 100 kA were additionally taken into account as great-current CG lightning, and marked as CG_{50}, CG_{75} and CG_{100} lightning, respectively.

TRMM satellite was launched on 28 November 1997, carrying the Lightning Imaging Sensor (LIS), Precipitation Radar (PR), TRMM Microwave Imager (TMI), Visible and InfraRed Scanner (VIRS) and Cloud and Earth Radiant Energy Sensor (CERES). The LIS Gridded Lightning Climatology Data was used to demonstrate the total lightning activity in analysis region. The specific style of the data and its feature in this dataset were described by Daniel et al. [2014]. It should be noted that this gridded climatology data is calculated based on the LIS observation and was not consistent with the CG data in years. The time of the data referred by LIS gridded climatology data should cover that of the CG data. But, because we considered the climatic statistics, the spatial-temporal characteristics should be comparable. The TRMM 3B43 dataset, i.e., TRMM and Other Data Precipitation Product, was used to exhibit the monthly precipitation with grid size of 0.25 degree.

ERA-interim data provided the monthly means of reanalysis meteorological field and helped to understand the correlation of the lightning activity and meteorological parameters. The data with grid size of 0.75 degree was chosen.

The analysis region and its terrain are shown in Figure 1. The analysis region was delineated by the red line. Part of the South China Sea adjoining Guandong is also included. But we limited the range of the included sea (the edge was basically within 150 km of GLLS network), in order to ensure the reliable detection efficiency of GLLS over it. The lightning activity in land and that in offshore water will be compared in paper. A total of about 244,000-km^2 area, including about 180,000-km^2 land and 64,000-km^2 offshore water, is covered by this region.

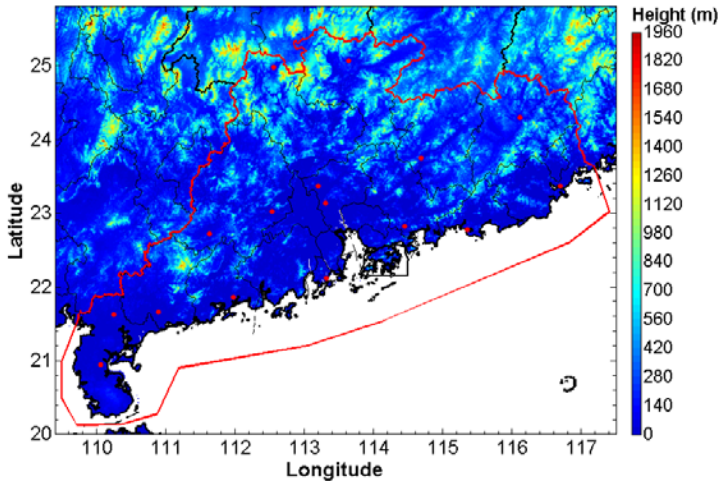

Fig. 1 The analysis region (delineated by the red curve) and the positions of GLLS sensors superposed on the color map showing the terrain. The red curve on the land describes the land part of the Guangdong administrative boundary.

LIGHTNING ACITIVITY AND ITS LAND-SEA DIFFERENCE

Spatial distribution

LIS High Resolution Full Climatology data (0.5-degree grid size) and CG data (calculated in 0.1-degree grid size) are used to display the density of total lightning activity (Figure 2a) and total CG lightning activity (Figure 2b) in analysis region, respectively. Table 1 shows the statistics on the average characteristics of lightning activity in whole region, land and offshore water.

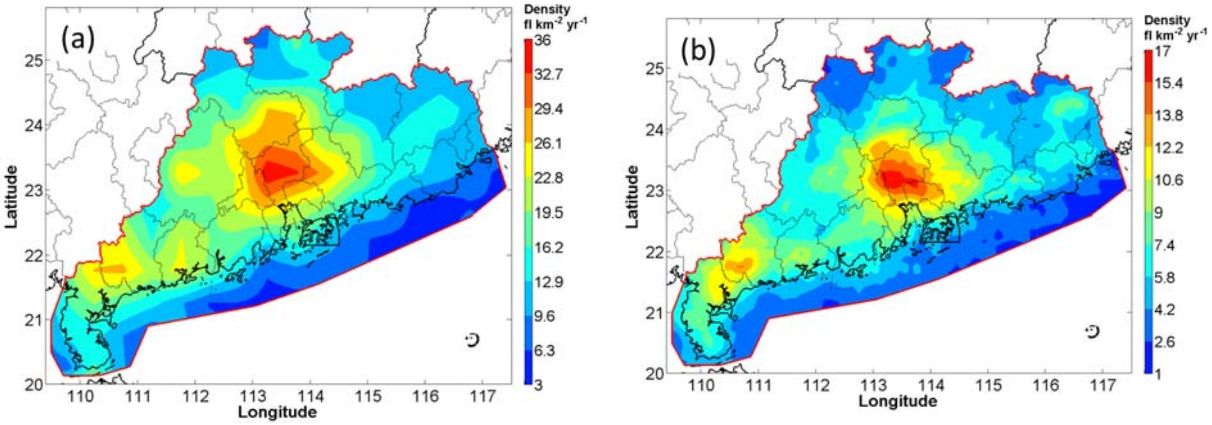

Fig.2 Density of total lightning (a) observed by TRMM/LIS and total CG lightning (b) observed by GLLS

Two regions with great lightning density (for both total lightning and total CG lightning) are exposed in Figure 2. One is located around the Pearl River Delta, centered at Guangzhou (near to (113.5E, 23N));

the other is located to the north of the Leizhou Peninsula (near to (110.5E, 21.75N)). If we compared the Figure 2 with Figure 1, it is found that these two regions are both half-surrounded by mountains, which is in favor of the convergence of the wind and water vapour coming from the sea, and therefore a possible key reason responsible for active convection and lightning activity.

Table 1 Statistics of the lightning activity in analysis region

Statistical Parameters	Types of lightning	Whole region	Land	Offshore Water	V_{land}/V_{water}
Density (fl km^{-2} yr^{-1})	Total lightning	15.90	18.05	9.90	1.82
	Total CG lightning	6.45	7.32	4.05	1.81
	PCG lightning	0.54	0.59	0.39	1.51
	CG_{50} lightning	0.86	0.91	0.73	1.25
	CG_{75} lightning	0.33	0.34	0.33	1.03
	CG_{100} lightning	0.16	0.15	0.18	0.83
Ratio [a] (%)	Total CG lightning	40.60	40.54	40.92	0.99
	PCG lightning	8.37	8.10	9.73	0.83
	CG_{50} lightning	13.31	12.38	17.99	0.69
	CG_{75} lightning	5.19	4.59	8.21	0.56
	CG_{100} lightning	2.47	2.09	4.35	0.48
Average peak current (kA)	Total CG lightning	30.48	29.85	37.01	0.81
	PCG lightning	34.50	33.11	40.14	0.82
	CG_{50} lightning	84.10	81.59	92.18	0.89
	CG_{75} lightning	120.83	117.84	128.55	0.92
	CG_{100} lightning	158.43	155.45	165.02	0.94

[a]: the ratio of total CG lightning is relative to total lightning, and other ratios of lightning is relative to total CG lightning.

Figure 2 explicitly shows that the lightning activity over the land is more vigorous than over the offshore water. Around the coastline, the density of lightning decrease steeply along the direction from land to sea. This situation is supported by the values listed in Table 1. Even the delineated sea region is so closed to the land, the density of lightning over land is near 2 twice that over offshore water. Meanwhile, when PCG lightning and great-current CG lightning are taken into account, the multiples decrease, until smaller than 1 for CG_{100} lightning.

In addition, the Table 1 explores that the ratio of total CG lightning to total lightning is almost similar over land and offshore water. Referring to the ratio values, we can calculate the *z* value over analysis

region is about 1.46, which is within the interval of 1.1—3.8 for latitude ranging from 20º to 40º reported by Mackerras and Darvenize [1994], but greater smaller than that for approximate latitude belt suggested by Prentice and Mackerras [1977] and Mackerras et al. [1998] (around 3—4). We further find the ratios of PCG lightning and great-current CG lightning to the total CG lightning over land are clearly smaller than those over offshore water. The grater of the peak current of the CG lightning, the more distinct the difference of the ratios between over land and over offshore water is. Furthermore, all kinds of CG lightning over the land have smaller peak current than those over offshore water.

Temporal variation

1) Monthly variation

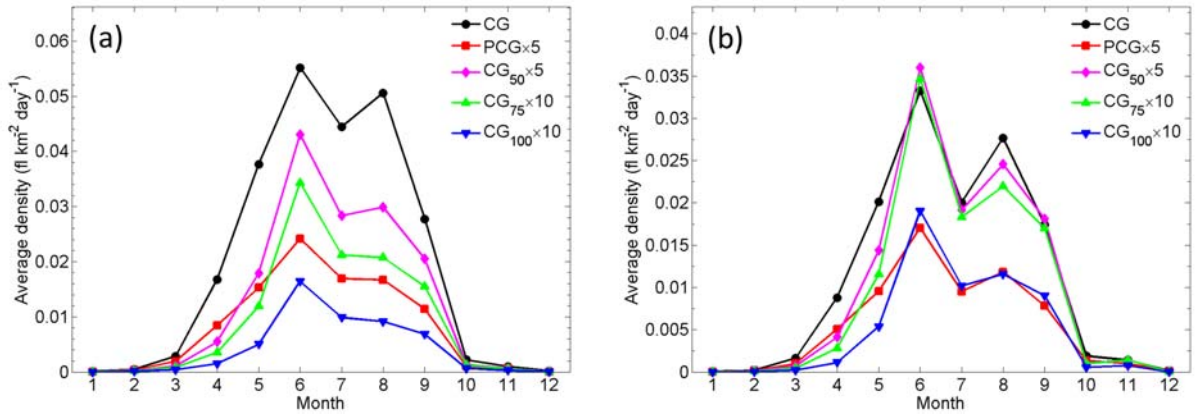

Fig.3 Monthly variation of CG lightning activity over land (a) and over offshore water (b). (in order to clearly show the variation in same axis, the values of part types of CG lightning are multiplied by factors; the same to below)

Figure 3 shows the monthly variation of CG lightning flashes. Most of them occur during the period from May to September. No matter over the land or the offshore water, the total CG lightning has two peaks corresponding to June and August. The lightning activity in June is more outstanding, especially for that over offshore water. An abrupt decrease of lightning activity occurs in July, which might be attributed to the relative steady weather caused by subtropical high over the analysis region around this month. Interestingly, the PCG lightning and great-current CG lightning over land only exhibit one main peak in June, while those over offshore water have two peaks similar to the total CG lightning.

Table 2 shows the ratios of PCG lightning and great-current CG lightning in different seasons. We refer to the seasonal division reported by Jian [1994], which is just consistent with the monthly distribution of lightning activity. It is found that the ratio of PCG lightning is relatively small in summer

and large in other seasons. Meanwhile, the ratios of great-current CG lightning are relatively large in summer and small in other seasons.

Table 2 Ratios of PCG lightning and great-current CG lightning to total CG lightning in different seasons.

regions	Types of lightning	Summer (from May to September)	Other seasons (from October to April of the second year)
Land	PCG lightning	7.87%	10.43%
	CG_{50} lightning	12.88%	7.67%
	CG_{75} lightning	4.76%	3.26%
	CG_{100} lightning	2.16%	1.56%
Offshore water	PCG lightning	9.35%	15.27%
	CG_{50} lightning	18.71%	9.07%
	CG_{75} lightning	8.59%	3.95%
	CG_{100} lightning	4.57%	1.99%

2) Diurnal variation

Distinct difference of diurnal variation of CG lightning between over land and over offshore water can be found in Figure 4 (a) and (b). Over the land, the lightning activity has only one peak in the period from 1600 to 1700 (local time), with vigorous lightning activity occurring from 1200 to 2100. However, the lightning activity over offshore water has two peaks in the period from 0700 to 0800 and the period from 1700 to 1800, respectively. Correspondingly, there are two time intervals with vigorous lightning activity; one is from 0300 to 0900, the other is from 1400 to 2100. Interestingly, the main peaks of the PCG lightning and great-current CG lightning are in the morning, while the main peak of the total CG lightning is in the afternoon.

The diurnal variation of the ratios of PCG lightning and great-current CG lightning is shown in Figure 4 (c) and (d). No matter over land or over offshore water, the smallest values occur in the afternoon, which is contrary to the lightning activity. Furthermore, the differences between peak and valley values of great-current CG lightning over offshore water are more distinct than those over land, the ratios of peak value to valley value for CG50, CG750 and CG100 being 1.76, 2.19 and 2.38 respectively over offshore water and 1.34, 1.75 and 2.14 respectively over land. These ratios also explore that the difference between peak and valley values increase with the increase of peak current of lightning.

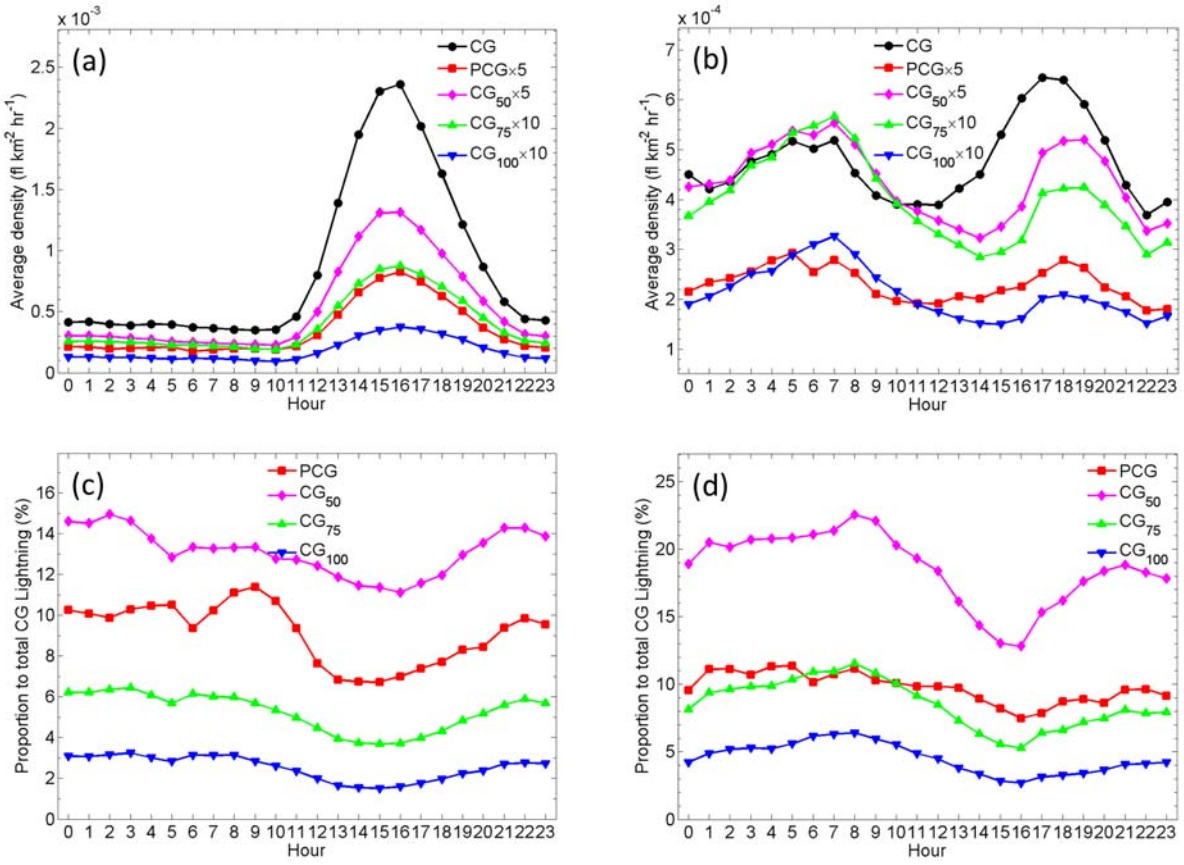

Fig.4 Diurnal variation of CG lightning activity over land (a) and over offshore water (b), and diurnal variation of ratios of PCG lightning and great-current CG lightning over land (c) and over offshore water (d). (the time labelled in x axes mean the period of an hour)

3) Diurnal variation in different seasons

Figure 5 explores that the diurnal variation of CG lightning activity changes with seasons. In summer, the total CG lightning activity over land has one peak in the afternoon, while in other seasons, there are two peaks occurring in the morning and afternoon, respectively. With regard to the total CG lightning over offshore water, there are two peaks occurring in the morning and afternoon, respectively, in summer, and one peak occurring in afternoon in other seasons. Furthermore, the diurnal variation of the great-current CG lightning in winter seems to be steady both over land and offshore water in other seasons.

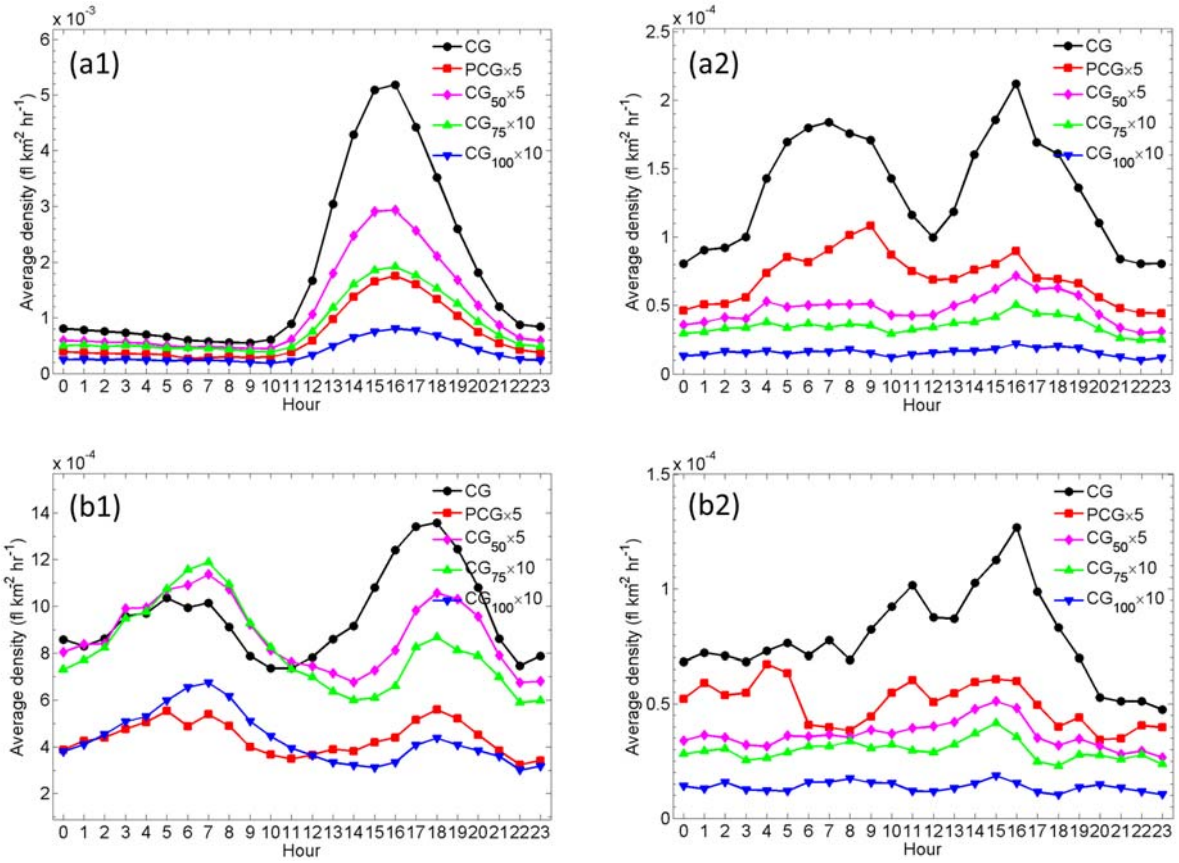

Fig.5 Diurnal variation of CG lightning activity over land and offshore water in different seasons. (a1): over land in summer; (a2) over land in other seasons; (b1): over offshore water in summer; (b2) over offshore water in other seasons.

RELATION BETWEEN LIGHTNING AND PRECIPITATION

Spatial correlation

Figure 6 exhibits the spatial distribution of average precipitation calculated from TRMM 3B43 data in analysis region. Comparing Figure 6 with Figure 2, we can find the distribution of precipitation is different from those of the total lightning or total CG lightning, which implies that the spatial correlation between them is weak. This situation might be attributed to diversity of the precipitation system in south China. Just as some studies reported [e.g. Sheridan et al. 1997; Petersen and Rutledge 1998; Soriano 2001; Zheng et al., 2012], the relationship between precipitation and lightning is relatively strong in dry areas and weak in wet areas.

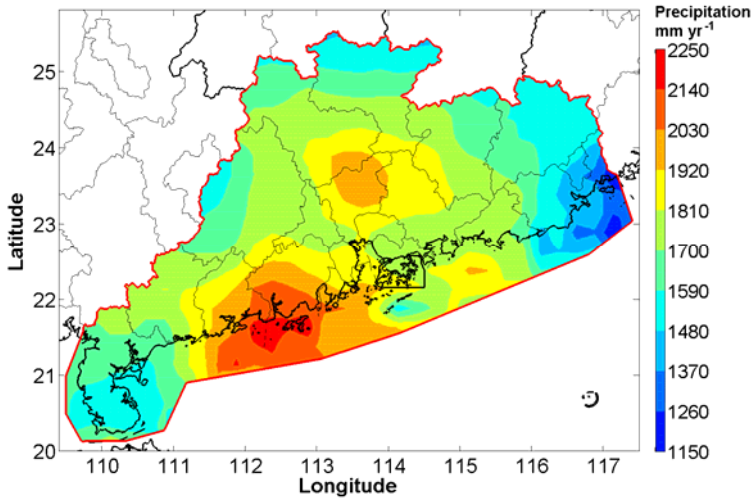

Fig.6 spatial distribution of average precipitation calculated from TRMM 3B43 data in 0.25-degree grids

However, when we separately consider the relationships of precipitation with different types of CG lightning, it is found that the correlation enhances with the increase of the current of CG lightning. Table 3 exhibits the correlation coefficients (*R*). It is clear that most outstanding correlation occurs between CG_{100} lightning and precipitation, whose scatters and fitted lines are shown in Figure 7. Furthermore, the correlations are relatively prominent in summer, and weak in other seasons.

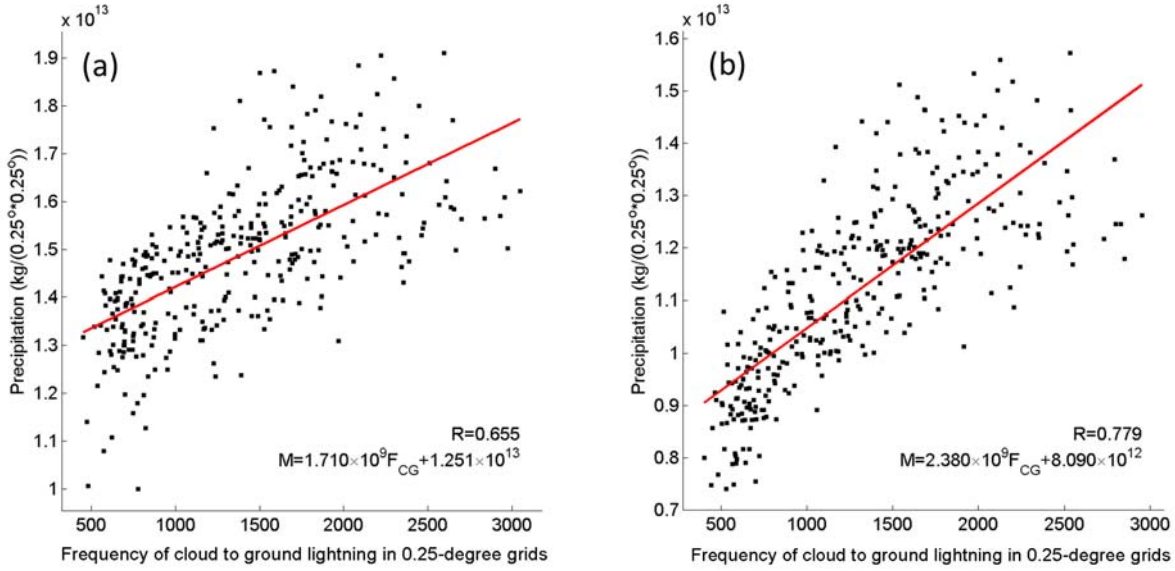

Fig.7 scatters and fitted lines representing the correlation between CG100 lightning and precipitation in full year (a) and summer (b)

Table 3 Correlation of precipitation with different types of CG lightning

Types of CG lightning	Total CG lightning	PCG lightning	NCG lightning	CG50 lightning	CG75 lightning	CG100 lightning
R	0.281	0.480	0.258	0.523	0.612	0.655
R in summer	0.306	0.564	0.278	0.586	0.715	0.779
R in other seasons	0.088	-0.157	0.115	-0.077	-0.121	-0.092

Rain-yields per flash (RPF)

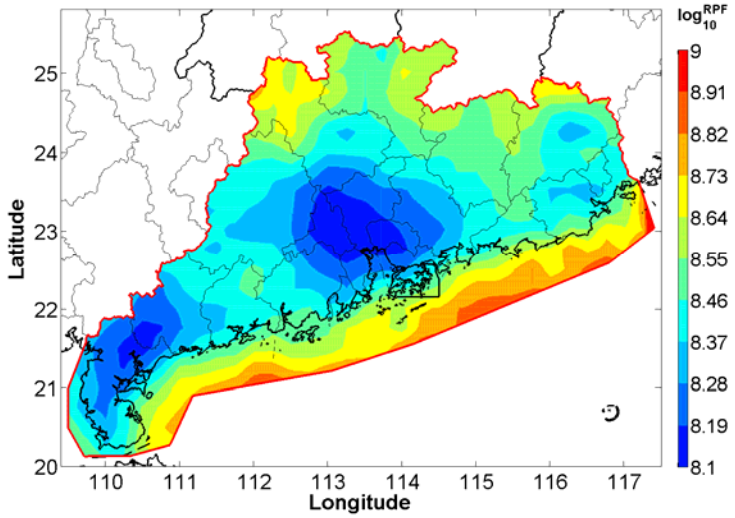

Fig.8 Spatial distribution of RPF (the value is the base-10 logarithm of RPF)

RPF is a frequently-used parameter in investigating the relationship between lightning and precipitation. We calculation this parameter in analysis region and show its spatial distribution in Figure 8. It is explored that the RPF is of the order of 10^8 kg fl^{-1}, which is close to the value of midcontinental United States documented by Petersen and Rutledge [1998].

Comparing Figure 8 and Figure 2, we can find there is a reversed relation between the distribution of density of lightning and that of RPF. In the storm-scale studies, some authors [e.g., Lopez et al. 1991; Williams et al., 1992; Zipser 1994] reported that the RPF value increase when the thunderstorms yielded more lightning. The spatial distribution of RPF supports this statement. In order to describe this reversed relation, we have attempted some functions and find the power function is the best one with R=-0.969. Figure 9 gives the scatter and fitted line representing the spatial correlation between density of total CG lightning and RPF.

We further investigate the difference of the average RPFs between the land and offshore water, and find the value of 4.67×10^8 kg fl^{-1} in the offshore water, which is about 1.77 times that in the land ($2.64\times$

10^8 kg fl^{-1}).

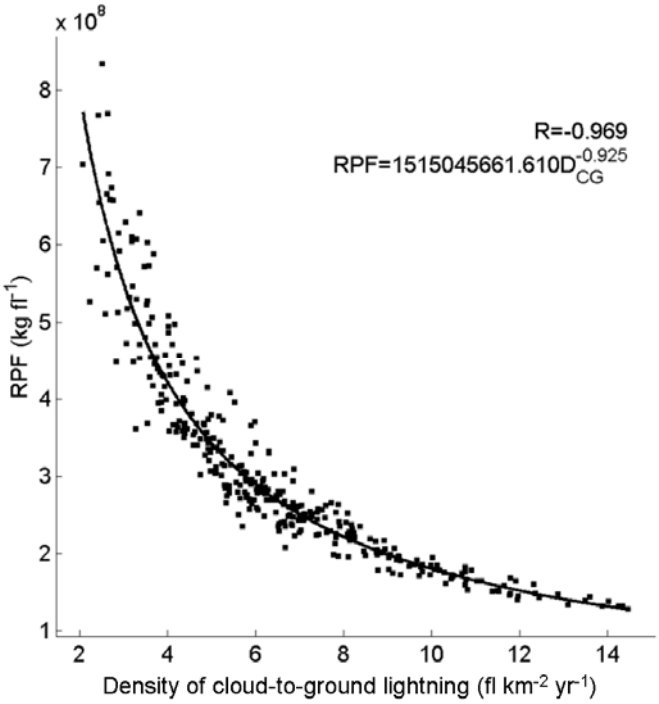

Fig. 9 scatter and fitted line representing the correlation between density of total CG lightning and RPF.

RELATION BETWEEN LIGHTNING AND METEOROLOGICAL PARAMETERS

The meteorological parameters provided by or calculated based on the data of ERA Interim Monthly Means of Daily Means on surface and pressure levels are referred here to investigate their relationships with the lightning activity in monthly variation in each 0.75-degree grid. This is an on-going work and only the preliminary results are exhibited.

Convective Available Potential Energy (CAPE) shows the most outstanding relationship with the lightning activity among the parameters associated with the atmosphere stratification. We attempted several functions to describe the relationship between lightning and CPAE, and show the frequently-used linear function and the best-fitting power function in Fig. 10. In linear relation, the correlation coefficient values are clearly greater in the land than those in the offshore water. When we turn to the power function, the correlation coefficient values in the whole analysis region rise significantly and are popularly above 0.8. Furthermore, the correlation is relatively even in whether the land and the offshore water.

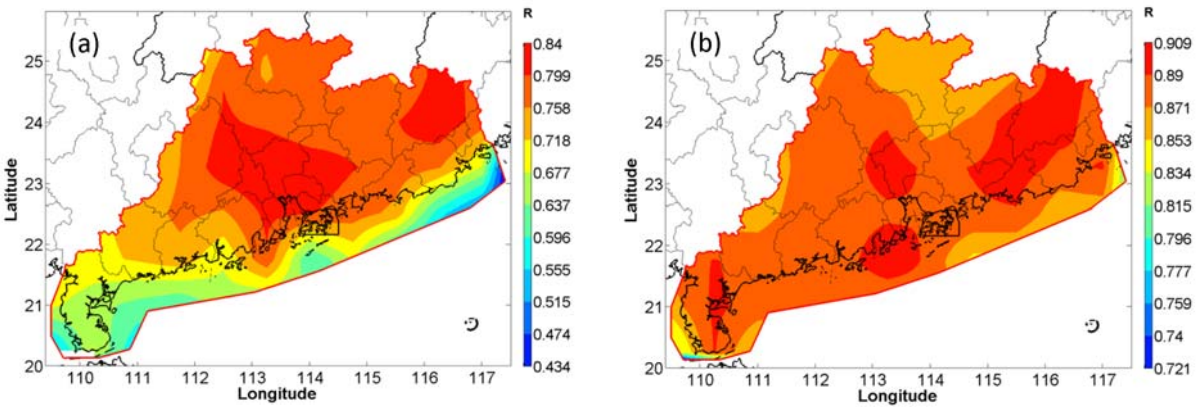

Fig.10 The distribution of the correlation coefficient of the linear-function relationship (a) and power-function relationship (b) between CAPE and lightning

CONCLUSIONS

Using the CG data observed by GLLS, total lightning and precipitation data observed by TRMM and the meteorological reanalysis date of ERA, we studied the lightning activity and its relations with meteorological parameters in South China and obtain the following results.

Two areas with half-surround terrain are found to have he most vigorous lightning activity in analysis region. The density of total CG lightning over land is near 2 twice that over offshore water, but for PCG lightning and great-current CG lightning, the multiple values decrease. The density of CG_{100} lightning over land is even smaller than that over offshore water. The z value is about 1.46 in whole region and relatively steady over land and offshore water. The ratios of PCG lightning and great-current CG lightning to the total CG lightning over land are clearly smaller than those over offshore water. All kinds of CG lightning over land have smaller average peak current than those over offshore water.

Most of the lightning occurs during the period from May to September with two peaks corresponding to June and August. The PCG lightning and great-current CG lightning over land only exhibit one main peak in June, while those over offshore water have two peaks similar to the total CG lightning. The ratio of PCG lightning is relatively small in summer and large in other seasons. Meanwhile, the ratios of great-current CG lightning are relatively large in summer and small in other seasons.

The lightning activity over the land has only one peak in the period from 1600 to 1700 (local time), while that over offshore water has two peaks in the period from 0700 to 0800 and the period from 1700 to 1800, respectively. Furthermore, the main peaks of the PCG lightning and great-current CG lightning over offshore water occur in the morning, while the main peak of the total CG lightning occur in the afternoon. The diurnal variations of the ratios of PCG lightning and great-current CG lightning are contrary to that of

the CG lightning, with their smallest values occurring in afternoon. The differences of ratios between peak and valley values of great-current CG lightning over offshore water are more distinct than those over land. In summer, the total CG lightning activity over land has one peak in the afternoon, while in other seasons, there are two peaks occurring in the morning and afternoon, respectively. On the contrary, the total CG lightning over offshore water has two peaks occurring in the morning and afternoon, respectively, in summer, and one peak occurring in afternoon in other seasons.

The total CG lightning activity has weak spatial correlation with precipitation. However, we find that the correlation enhances with the increase of the current of CG lightning. For CG_{100} lightning, the correlation coefficient is 0.779 in summer. The RPF in whole region is of the order of 10^8 kg fl^{-1}, which is close to the value of midcontinental United States. The average RPF in the offshore water (4.67×10^8 kg fl^{-1}) is about 1.77 times that in the land (2.64×10^8 kg fl^{-1}). A prominent reversed relation between the spatial distributions of density of lightning and that of RPF is exposed. It can be best described by the power function with the correlation coefficient of -0.969.

CAPE shows the most outstanding relationship with the lightning in monthly variation among the meteorological parameters associated with atmospheric stratification. When we refer to the linear correlation, the relationship is clearly strong in the land and weak in the offshore water. The power-function correlation is better, with the correlation coefficients being popularly above 0.8 in whole region and relatively even in whether the land and the offshore water.

ACKNOWLEDGMENTS

This work is supported by Basic Research Fund of Chinese Academy of Meteorological Sciences (Grant No. 2013Z006) and National Key Basic Research Program of China (2014CB441402).

The authors would like to acknowledge European Center for Medium-Range Weather Forecasts (ECMWF) who provided the ERA-interim reanalysis data.

The data of total lightning and precipitation were acquired as part of the Tropical Rainfall Measuring Mission (TRMM). The algorithms were developed by the TRMM Science Team. The data were processed by the TRMM Science Data and Information System (TSDIS) and the TRMM Office; they are archived and distributed by the Goddard Earth Sciences Data and Information Services Center (GES DISC). TRMM is an international project jointly sponsored by the Japan National Space Development Agency (NASDA) and the U.S. National Aeronautics and Space Admin- istration (NASA) Office of Earth Sciences.

REFERENCES

Chen, L., Y. Zhang, W. Lu, D. Zheng, Y. Zhang, S. Chen, and Z. Huang, 2012: Performance Evaluation for a Lightning Location System Based on Observations of Artificially Triggered Lightning and Natural Lightning Flashes. J. Atmos. Oceanic Technol., 29(12), 1835-1844.

Chen. S., Y. Du, L. Fan, H. He, and D. Zhong, 2002: Evaluation of the Guang Dong lightning-location system with transmission line fault data. Proc. Inst. Elect. Eng., Sci. Meas. Technol., 149(1), 9-16.

Cummins, K. L., M. J. Murphy, E. A. Bardo, W. L. Hiscox, R. B. Pyle and A. E. Pifer, 1998: A combined TOA/MDF technology upgrade of the U.S. National Lightning Detection Network. J. Geophys. Res., 103(D8), 9035-9044.

Daniel, J. C., E. B. Buechler, and J. B. Richard, 2014: Gridded lightning climatology from TRMM-LIS and OTD: Dataset description. Atmos. Res., 135-136, 404-414.

Jian, M., 1994: The division of seasons for the South China region. Acta Scientiarum Naturalium Universitatis Sunyatseni, 33(2), 131-133 (in Chinese).

López, R. E., R. Ortíz, W. D. Otto, and R. L. Holle, 1991: The lightning activity and precipitation yield of convective cloud systems in central Florida. Preprints, 25th International Conf. on Radar Meteorology, Amer. Meteor. Soc., 907-910.

Mackerras D., and M. Darveniza, 1994: Latitudinal variation of lightning occurrence characteristics. J. Geophys. Res., 99(D5), 10813-10821.

MacKerras, D., M. Darveniza, R. E. Orville, E. R. Williams, and S. J. Goodman, 1998: Global lightning: total, cloud and ground flash estimates. J. Geophys. Res., 103(D16), 10813-10821.

Petersen, W. A. and Rutledge S. A., 1998: On the relationship between cloud-to-ground lightning and convective rainfall. J. Geophys. Res., 103(D12), 14025-14040.

Prentice, S. A., and Mackerras D., 1977: The ratio of cloud to cloud-ground lightning flashes in thunderstorms. J. Appl. Meteor., 16, 545-550.

Sheridan, S. C., J. F. Griffiths, and R. E. Orville, 1997: Warm Season Cloud-to-Ground Lightning–Precipitation Relationships in the South-Central United States. Wea. Forecasting, 12, 449–458.

Soriano, L. R., F. de Pablo, E. G. Díez, 2001: Relationship between Convective Precipitation and Cloud-to-Ground Lightning in the Iberian Peninsula. Mon. Wea. Rev., 129, 2998–3003.

Williams, E. R., S. A. Rutledge, S. G. Geotis, N. Renno, S. A. Rutledge, E. Rasmussen, T. Rickenbach, 1992: A radar and electrical study of tropical “hot towers”. J. Atmos. Sci., 49, 1386-1395.

Zheng, D., J. Dan, Y. Zhang, C. Wu, C. Zeng, 2012: Regional differences of relationship between cloud-to-ground lightning and precipitation in China. J. Tropical Meteor., 28(4), 569-576.

Zipser, E. J., 1994: Deep cumulonimbus cloud systems in the tropics with and without lightning. Mon. Weather Rev., 122, 1837-1851.